Well Clear Trade Study for Unmanned Aircraft System Detect And Avoid with Non-Cooperative Aircraft

Minghong G. Wu * and Andrew C. Cone †
NASA Ames Research Center, Moffett Field, CA 94035, USA

Seungman Lee ‡
Crown Consulting Inc., NASA Ames Research Center, Moffett Field, CA 94035, USA

Christine Chen§ and Matthew W. M. Edwards ¶
Lincoln Laboratory, Massachusetts Institute of Technology, Lexington, MA 02420, USA

Devin P. Jack ‖
Adaptive Aerospace Group, Inc., Hampton, VA 23666, USA

This paper presents a process for selecting candidate Detect-and-Avoid Well Clear definitions for Unmanned Aircraft Systems and non-cooperative aircraft. The selection is based on considerations of the unmitigated collision risk, maneuver initiation range, and others. Operational assumptions related to low cost, size, weight, and power sensors equipped by the Unmanned Aircraft Systems are applied to set the scope of aircraft performance and drive metrics computation. Four candidate Well Clear definitions, two primary and two secondary, varying from 1500 to 2500 ft in their horizontal miss distance and from 0 to 25 sec in modified tau, are selected for future analyses.

Nomenclature

ACES	Airspace Concept Evaluation System
AGL	above ground level
BADA	Base of Aircraft Data
C-SWaP	cost, size, weight, and power
DAA	detect and avoid
DWC	DAA well clear
FAA	Federal Aviation Administration
D_{mod}	distance modification
HMD	horizontal miss distance
IFR	instrument flight rules
LoDWC	loss of DWC
MIR	maneuver initiation range
MOPS	minimum operational performance standards
MSL	mean sea level
NMAC	near mid-air collision

*Research Engineer, Aviation Systems, AIAA member
†Research Engineer, Aviation Systems, AIAA member
‡Senior Research Scientist, Senior AIAA Member
§Associate Technical Staff, Surveillance Systems
¶Technical Staff, Surveillance Systems, Senior AIAA Member
‖Research and Development Engineer, AIAA Member

P	Unmitigated Collision Risk
RA	resolution advisory
RADES	radar evaluation squadron
SC-228	special committee 228
TCAS	Traffic Alert and Collision Avoidance System
TSO	Technical Standard Order
UAS	unmanned aircraft system
VFR	visual flight rules
h	altitude separation between two aircraft
r	range between two aircraft
$\dot{r}$	range rate
t	time
t_{pz}	time to protected zone
τ_{mod}	modified tau

I. Introduction

Detect and Avoid (DAA) Systems are a critical component for successful integration of Unmanned Aircraft System (UAS) operations in the National Airspace System (NAS). A DAA system provides surveillance, alerts, and guidance to keep a UAS "Well Clear" of other aircraft.[1,2] In the United States, simulation tests as well as flight tests have provided supporting information for defining a DAA Well Clear[1,3] (DWC) and requirements for the alerting and guidance performance.[4–7] Prototype DAA algorithms have also been developed to alerting and guidance research.[8–10] These developments enabled the RTCA Special Committee 228 (SC-228) to publish the Minimum Operational Performance Standards (MOPS) for DAA systems[11] and air-to-air radar[12] in 2017. The corresponding Technical Standard Orders (TSO), TSO-C211 and TSO-C212, were published by the Federal Aviation Administration (FAA) in October 2017. These standards, referred to as the Phase 1 MOPS, target UAS operations in non-terminal areas. UAS shall be equipped with surveillance systems containing Automatic Dependent Surveillance-Broadcast (ADS-B) In, airborne active surveillance, and air-to-air radar that can detect aircraft without transponders. Traffic Alert and Collision Avoidance System (TCAS) II[13] is an optional component. Phase 2 work for extending the MOPS to additional UAS categories and operations is underway.

One of the Phase 2 MOPS objectives is to enable operations for UAS equipped with low cost, size, weight, and power sensors (low C-SWaP). These UAS missions are envisioned to take place at altitudes below 10,000 ft MSL with UAS speeds much lower than 200 kts, the maximum UAS airspeed in the Phase 1 MOPS. For these UAS and their missions, a large and high-power radar required by the Phase 1 radar MOPS is physically infeasible and/or economically impractical. Missions falling in this category include air quality monitoring, aerial imaging and mapping, and flood inundation mapping.[14] Compared to the radar meeting the Phase 1 MOPS, low C-SWaP sensors provide less range for the UAS to detect and remain Well Clear from aircraft without transponders, i.e., non-cooperative aircraft. To find a path to enable these operations, assumptions and performance metrics utilized in Phase 1 MOPS are re-examined in Phase 2 work.

One of the Phase 1 requirements reexamined in Phase 2 is the DWC definition. Phase 1 DWC was driven largely by interoperability with TCAS II. The form and size of the DWC were chosen such that the DWC encloses almost the entire volume inside which TCAS II would issue Resolution Advisories (RA). TCAS cannot detect non-cooperative aircraft, and therefore the TCAS RA consideration is irrelevant for non-cooperative aircraft, for which the Phase 1 DWC volume is likely to be unnecessarily large. It is desirable by SC-228 to seek an alternative DWC definition between an UAS and non-cooperative aircraft. The UAS considered include both those with low C-SWaP sensors and UAS defined in the Phase 1 MOPS (carrying a high-power radar). The alternative DWC does not necessarily take the same form as the Phase 1 MOPS DWC. It is, nonetheless, expected to be smaller than the Phase 1 DWC.

As a direct support of SC-228 Phase 2 MOPS work, this paper presents a trade study of potential DWC definitions using two metrics related to loss of DWC (LoDWC). The two metrics are the unmitigated collision risk and the maneuver initiation range. Multiple types of DWC are explored and results are compared. Low C-SWaP operations are assumed for computing the metrics, although the resulting candidate DWCs are expected to be applicable to Phase 1 UAS as well. Section II briefly reviews the approach adopted in Phase

1 for selecting a DWC. The approach in this work is described in Section III. Section IV describes the two encounter sets used for computing the unmitigated collision risk. The maneuver initiation range is described in Section V. Results are presented in Section VI, and the down-selection process is discussed in Section VII.

II. Background

The DWC in Phase 1 was initially selected from three types of DWC definitions using eight performance metrics.[1] The unmitigated collision risk, denoted as P, was used for tuning the DWC threshold parameters so that all three DWCs yield the same value of P.[1] P stands for the conditional probability of a near mid-air collision (NMAC) given a LoDWC without mitigation (by ownship maneuver):

$$P = P(\text{NMAC}|\text{LoDWC}) \tag{1}$$

An earlier study recommended a P value of 5% for consideration of a DWC.[15] During the Phase 1 MOPS work, the target value of P was set to 1.5% initially so as to expand the DWC volume to enclose most of the TCAS II Resolution Advisory alerting volume.[1] The selected DWC, however, had an undesirable vertical separation threshold of 700 ft, above the vertical separation of 500 ft required by visual flight rules (VFR).[3] The vertical separation threshold was changed to 450 ft, and the final DWC resulted in a P of 2.2%.

Maneuver initiation range (MIR) was one of the eight performance metric considered in Phase 1 MOPS.[16] It is defined by a stressing case of head-on encounter, as the range between aircraft when the UAS must start maneuvering away in order to maintain DWC. Constant heading rate turns are assumed for horizontal maneuvers and constant climb and descent rates for vertical maneuvers.

The other performance metrics adopted in the Phase 1 DWC selection process are not considered for this work. Some of these metrics are irrelevant (TCAS interoperability for example), and some others require additional assumptions about an alerting and guidance algorithm that would make it hard to tie the results directly to the DWC.

The DWC in Phase 1 does not map to distinct physical boundaries because it depends on two aircraft's relative position and velocity. Figure 1 illustrates a DWC zone defined by the three parameters. The Horizontal Miss Distance (HMD) represents the two aircraft's predicted minimum horizontal distance (in the future) assuming constant velocities. The parameter h represents the two aircraft's current altitude difference. The time metric modified tau, τ_{mod}, is an estimated time taken for the two aircraft to get horizontally close to each other. The thresholds, denoted by an asterisk, for the HMD, h, and τ_{mod} are 4000 ft, 450 ft, and 35 sec, respectively. All three parameters must simultaneously fall below their respective thresholds during an encounter for the two aircraft to violate the DWC.

The use of HMD and τ_{mod} in a DWC definition was meant to facilitate interoperability with TCAS II, which uses similar definitions of HMD and τ_{mod} in its alerting algorithm. The definition of τ_{mod} is[2]

$$\tau_{mod} = \begin{cases} -\frac{r^2 - {D_{\text{mod}}}^2}{r\dot{r}}, r > D_{\text{mod}}, \\ 0, r \leq D_{\text{mod}} \end{cases} \tag{2}$$

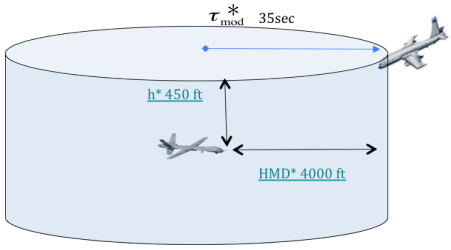

Figure 1. A schematic representation of the DWC zone.

where r and $\dot{r}$ are the horizontal range and range rate between the intruding aircraft (referred to as the intruder) and the UAS (referred to as the ownship), respectively. The range rate is negative for closing geometries. The distance modification D_{mod} defines the radius of a protection disk around the ownship such that any intruder with a horizontal range less than D_{mod} is always considered an urgent threat. In this case, $\tau_{mod} = 0$.

III. Approach

This trade study aims to recommend candidate DWC definitions for the SC-228 to consider. The envisioned workflow diagram is shown in Figure 2. The independent variable is a DWC definition,

shown at the top of this diagram. Each DWC is defined by a set of threshold parameters. Encounters between UAS and non-cooperative aircraft, generated from simulations or models with representative distributions, are analyzed to estimate P. The simulation suites for generating encounters are the Airspace Concept Evaluation System (ACES)[17] and MIT Lincoln Laboratory's uncorrelated encounter model.[18] Target values of P(NMAC|LoDWC) are applied to down-select DWC definitions. The 2-degree-of-freedom Prototyping Airplane Interaction Research Simulation (2PAIRS)[19] is used to compute the MIR. Section IV describes the simulation setup in details.

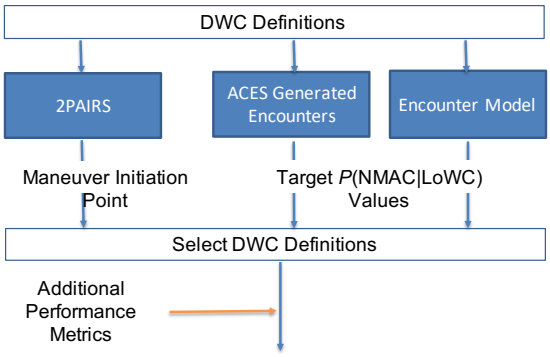

Figure 2. Workflow

A few variables that set the scope of the low C-SWaP operations considered, and likewise the scope of the encounter data considered, are given here:

- Extended UAS operations in non-terminal Classes D, E, and G airspaces, as well as those occurring during transit UAS operations in Classes B and C airspaces, are considered.
- Encounters above 500 ft AGL and below 10,000 ft mean sea level (MSL) are considered. The upper bound of 10,000 ft comes from the FAA's rule that requires Mode C transponders for aircraft flying above 10,000 ft MSL.
- Encounters in which the non-cooperative aircraft's airspeed is at or below 170 kts (95% percentile[20]) are considered.
- UAS speed range is between 40 and 100 kts.

The types of DWC definitions considered are described in Table 1. Here t_{pz} is the predicted time to protected D_{mod} disk.[21] This time metric corresponds to a physical event and changes linearly with time during a non-accelerating encounter. Compared to τ_{mod}, t_{pz} can be potentially a better time component for DWC or alerting algorithms. DWC3 is a conventional static cylinder adopted by air traffic control as a type of separation standard. DWC4 is a dynamic cylinder that is conceptually simpler than DWC1 and DWC2 because it does not have a HMD threshold. Note DWC3 is the limiting case of other DWC types when their time component reduces to zero.

Table 1. Types of DWC considered

Type	Parameters	LoDWC Condition	Comment
DWC1	h^*, HMD*, ${\tau_{mod}}^*$	$h < h^*$ and HMD $<$ HMD* and $\tau_{mod} < {\tau_{mod}}^*$	Phase 1 DWC
DWC2	h^*, HMD*, ${t_{pz}}^*$	$h < h^*$ and HMD $<$ HMD* and $t_{pz} < {t_{pz}}^*$	Alternative time metric
DWC3	h^*, r^*	$h < h^*$ and $r < r^*$	Static cylinder
DWC4	h^*, r^*, t^*	$h < h^*$ and $r < r^* - \min(\dot{r}, 0) \times t^*$	Dynamic cylinder

IV. Encounter Sets

IV.A. ACES Generated Encounters

Encounters are needed for this study for interactions between UAS (assumed to fly under IFR) and non-cooperative VFR aircraft that do not have a transponder. ACES fast-time simulation was used for generating UAS trajectories. ACES provides a capability to simulate NAS-wide, gate-to-gate air traffic operations at local, regional, and national levels with medium-fidelity aircraft flight dynamics models.[17] It simulates flight trajectories using aircraft models represented in a form similar to those from the Base of Aircraft Data (BADA).[22] Aircraft models tailored for Aerosonde Mark 4.7, Shadow RQ-7, Ikhana/Predator B, Reaper MQ-9, and Global Hawk have been implemented and verified in ACES.

For this study, an entire day's worth of UAS flights conducting 12 different types of missions considered suitable for UAS with low C-SWaP sensors are analyzed. The demand and mission profiles were generated based on subject matter experts opinions and socio-economical analysis.[14] Table 2 shows the 12 UAS missions. These missions amount to a total of 17,100 hours' flight time.

Table 2. Missions for UAS with low C-SWaP sensors

Mission Type	UAS Type	Cruise Altitude (AGL)	Cruise Speed (KTAS)	Flight Pattern
Aerial Imaging and Mapping	Aerosonde Mk 4.7	3000 ft.	44 to 51	Radiator-grid pattern or circular pattern
Air Quality Monitoring	Shadow(RQ-7B)/ NASA SIERRA[23]	4k, 5k, and 6k ft.	74 to 89	Radiator-grid pattern
Airborne Pathogen Tracking	Shadow(RQ-7B)/ NASA SIERRA	3,000 ft., 5,000 ft. and 10,000 ft.	72 to 97	Radiator-grid pattern
Flood Inundation Mapping	Aerosonde Mk 4.7	4,000 ft.	46 to 51	Grid pattern
Flood Stream Flow	Aerosonde Mk 4.7	4,000 ft.	46 to 51	Grid pattern and/or along stream direction
Law Enforcement	Aerosonde Mk 4.7	3,000 ft.	44 to 51	Three types of pattern: 1) grid pattern, 2) random, 3) outward spiral
Point Source Emission	Shadow(RQ-7B)	3,000 ft.	72 to 80	Grid pattern and/or along stream direction
Spill Monitoring	Shadow(RQ-7B)/ SIERRA	3,000 ft. to 13k ft. (at every 1,000 ft.)	72 to 93	Up and down-wind flights radiator-grid pattern, round-the-clock
Tactical Fire Monitoring	ScanEagle/ Shadow(RQ-7B)	3,000 ft.	72 to 75	Circular flight path following the perimeter of a wildfire
Traffic Monitoring	Shadow(RQ-7B)/ SIERRA	1,500 ft.	58 to 84	Geo-spatial monitoring flight path
Wildlife Monitoring	Aerosonde Mk 4.7	3,000 ft.	44 to 51	Radiator-grid pattern
News Gathering	Aerosonde Mk 4.7	1,500 ft. to 3,000 ft.	44 to 51	Random-path: e.g., police-chase; circular orbit:

For the intruder traffic, nation-wide VFR flight paths flown on 21 days in 2012 were extracted from the historical Air Force 84th Radar Evaluation Squadron (RADES) radar data. The RADES data include primary-only radar returns (for non-cooperative aircraft) as well as cooperative transponder returns, providing track updates every 5 or 12 seconds. The instrument flight rules (IFR) track data, i.e., those with non-1200 discrete transponder codes, were excluded from the analysis. This is because air traffic controllers have a responsibility for separating IFR aircraft from other IFR (including UAS) aircraft. The remaining VFR track data, including non-cooperative aircraft and those cooperative aircraft with 1200 transponder code were processed to remove measurement noise and generate continuous trajectory data.

Due to the limited number of non-cooperative VFR trajectories available, 1200-code cooperative VFR aircraft are used as a surrogate for non-cooperative aircraft. This is a reasonable approach since the flight characteristics of conventional non-cooperative aircraft are similar to those using a 1200-code cooperative VFR aircraft in terms of airspeed, acceleration, and turn rate.[18]

The encounters between UAS and VFR aircraft were simulated using SAA Control, a client of the Java Architecture for DAA Extensibility and Modeling (JADEM).[24] JADEM employs a model of a DAA system that provides functions to evaluate potential LoDWC, to declare a DAA alert, and to optionally execute a maneuver to avoid predicted LoDWC. In this study, both the UAS trajectories and the actual VFR flight tracks were played back from files to create encounters. No maneuvers were applied to the UAS to avoid LoDWC. To analyze only the encounters that fit the operational assumptions, the encounter data were filtered by the altitude and speed of ownship and intruder aircraft. Unmanned aircraft whose speed at the CPA is less than 100 kts, and altitude at the CPA is below 10,000 ft MSL and above 500 ft AGL, were selected. Non-cooperative intruder aircraft whose speed at CPA is less than 170 kts and altitude at CPA

is below 10,000 ft MSL and above 500 ft AGL were selected for the simulation results data analysis in this study.

A total of two million encounters were constructed from the UAS trajectories against 21 days of traffic data. Since all VFR traffic within a large volume of 20 nmi horizontal distance and 10,000 ft altitude with respect to an UAS are considered for encounters, only a small fraction of the encounters resulted in LoDWC. An even smaller fraction of encounters led to NMAC. A total of 500 NMACs were identified.

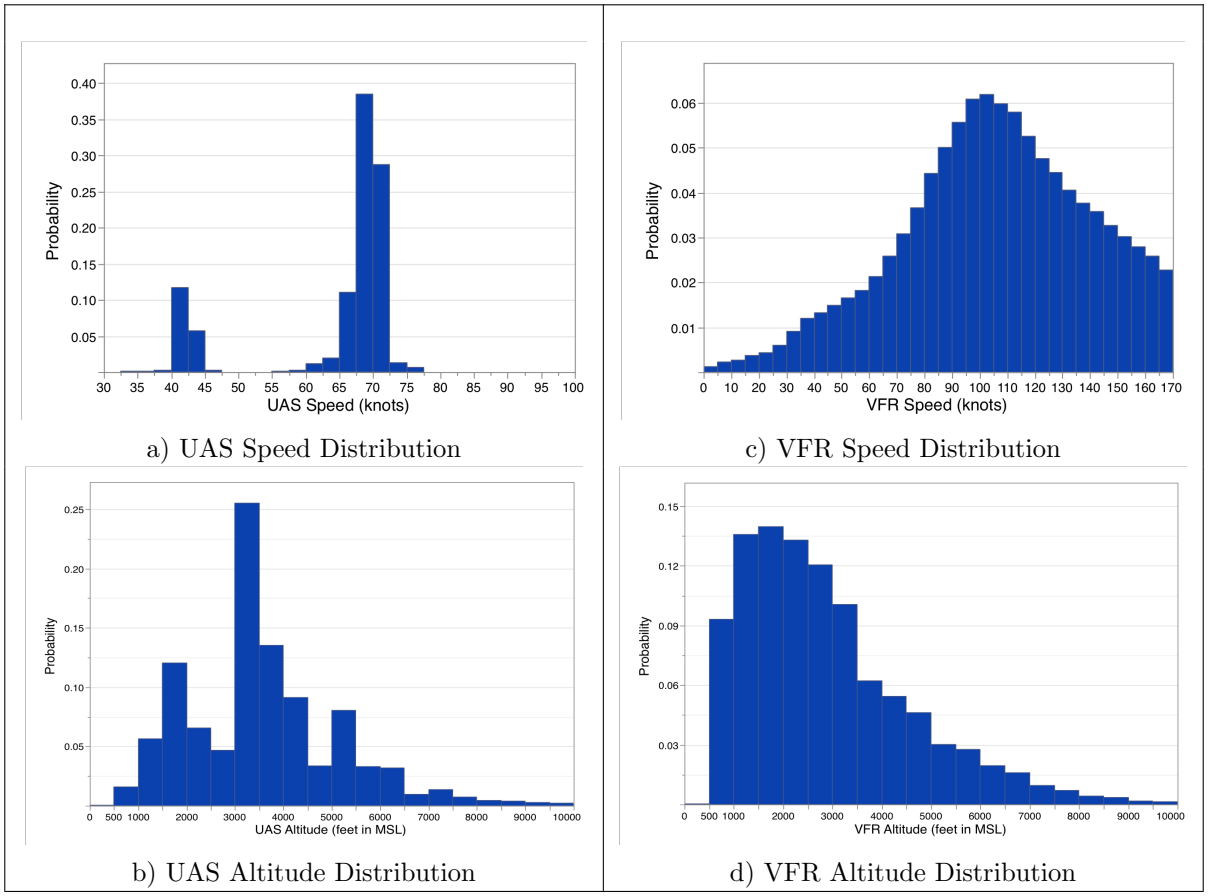

Figure 3. Speed and altitude distribution of UAS and VFR traffic

IV.B. Uncorrelated Encounter Model

The MIT Lincoln Laboratory's uncorrelated encounter model (referred to as the encounter model in the remainder of this paper) is used for this work to complement and validate results from the ACES generated encounters. This encounter model has been used in Phase 1 for tuning the parameters of candidate DWC types for a target P.[1] This model "is representative of encounters between a cooperative aircraft and a conventional non-cooperative aircraft similar those using a 1200 transponder code."[18,25] Bayesian networks are used to create random aircraft trajectories that are statistically representative of VFR trajectories observed from radar data. The radar data used for developing this model came from radar returns of 1200-code aircraft from over 200 RADES radar sites across the NAS. As with the VFR traffic used in generating ACES encounters, the 1200-code aircraft were used to represent similar, conventional non-cooperative aircraft due to the lack of altitude information for non-cooperative aircraft. Altitude estimation was based on Mode C transponder reports of pressure altitude from the same radar data.

The encounter model can be used to create trajectories up to 5 minutes before the closest point of approach, and so is well suited for studies involving collision avoidance and/or loss of separation for UAS encountering non-cooperative aircraft. The trajectories created from this model are also suitable for use in fast-time Monte Carlo simulations. The encounters are all pair-wise by default, but there is a capability for producing multiple aircraft encounters if required.

Since both the UAS and intruder trajectories are sampled from the same Bayesian networks, the UAS trajectory has the same characteristics as the intruder trajectory in terms of climb, descent, and turn rates. This distinguishes the encounter model from ACES encounters, in which UAS trajectories have different characteristics than the intruder trajectories because the UAS trajectories are constructed from flight data and specific aircraft performance models.

About one million encounters, defined when aircraft come within 3 nmi horizontally and 1000 ft vertically, were generated from the encounter model for the computation of P.

V. Maneuver Initiation Range

In addition to P computed from encounters, MIR is computed for each DWC definition using 2PAIRS.[16] The MIR is the distance between two aircraft when the UAS must maneuver away from the intruder to maintain DWC during a stressing head-on encounter. Figure 4 shows how an MIR is computed from a hypothetical, head-on encounter. Although the UAS maneuver can be horizontal, vertical, or a combination of both, only horizontal maneuvers are considered for this study. This is because vertical maneuvers are less robust in the presence of significant vertical surveillance errors typical for non-cooperative aircraft. A constant turn rate following a transient period of constant roll rate is used for modeling turns. It is assumed that smaller MIRs are preferable so as to potentially reduce the associated sensor requirements.

This work defines the MIR as the maximum value resulting from the range of UAS speed considered. Either the low speed of 40 kts or the high speed of 100 kts can be the stressing case.[26,27] It turns out that 40 kts MIR governs the low time metric (τ_{mod} or t_{pz} less than 20 sec) parameter space for DWC1 and DWC2. The 100 kts MIR governs the high time metric area of the contour.

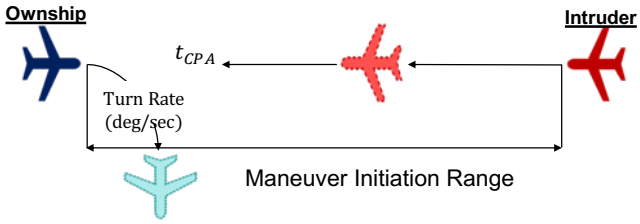

Figure 4. Head-on encounter and ownship maneuver considered for an MIR.

A turn rate of 7 deg/sec is considered suitable for the range of UAS speed (40 to 100 kts) and is thus assumed for modeling the UAS maneuver. This turn rate is higher than the standard turn rate of 3 deg/sec considered for Phase 1 UAS, which has a speed range of 40 to 200 kts. Increasing the turn rate beyond 7 deg/sec has diminishing returns in the UAS's ability to maintain WC[26] (meaning it hardly reduces the MIR further).

VI. Results

VI.A. Parameter Ranges

Table 3 lists ranges of DWC parameters considered for this work. No altitude separation other than $h^* = 450$ ft is explored, because raising h^* over the legal VFR traffic separation of 500 ft is not an option, and reducing h^* will undesirably drive the required horizontal separation up (and the associated sensor range requirements).

Table 3. Parameter space considered for DWCs

Type	Parameter Space
DWC1	$h^* = 450$ ft; HMD$^* \in [1000,\ 6000]$ ft; ${\tau_{mod}}^* \in [0,\ 35]$ sec
DWC2	$h^* = 450$ ft; HMD$^* \in [1000,\ 6000]$ ft; ${t_{pz}}^* \in [0,\ 35]$ sec
DWC3	$h^* = 450$ ft; $r^* \in [1000,\ 10000]$
DWC4	$h^* = 450$ ft; $r^* \in [1000,\ 6000]$ ft; $t^* \in [0,\ 35]$ sec

VI.B. Comparison of Encounter Sets

Figure 5 shows results of P computed from ACES encounters and from the encounter model. The computation is based on DWC1. The contours are produced by MATLAB from values of P at grid points. The contours agree well, with a difference of 0.1% or less for $\tau_{mod} < 25$. The difference increases slightly for larger values of τ_{mod}.

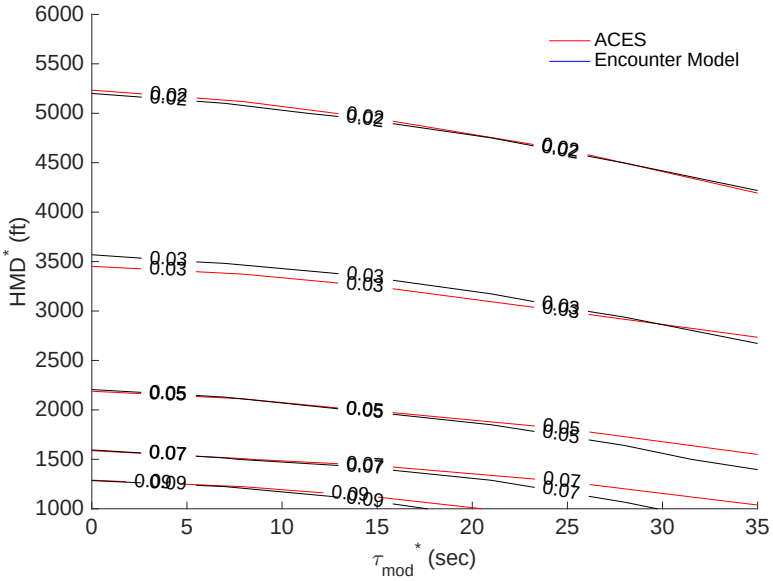

Figure 5. Unmitigated collision Risks computed from ACES encounters and the encounter model.

Figure 6 shows P computed using DWC3. The encounter model yields slightly higher values of P, although the values are very close.

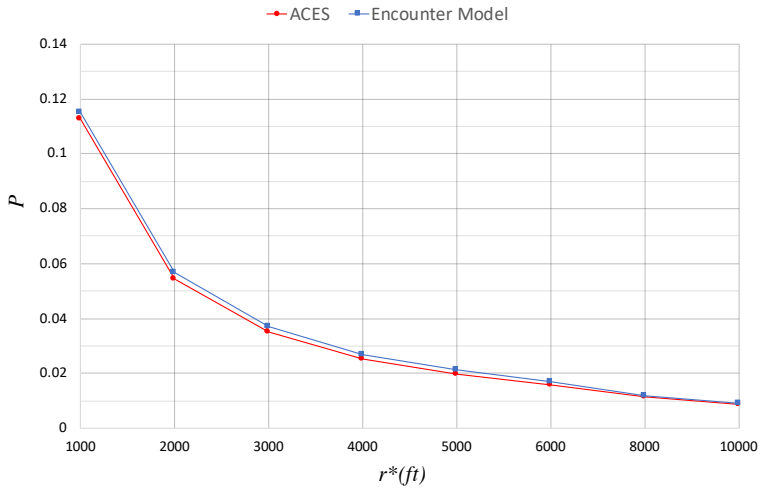

Figure 6. P for DWC3 from ACES encounters and the encounter model.

Although the VFR traffic from which intruder trajectories are sampled is similar in both sets of encounters, the UAS trajectories are different and, most likely, result in the slight difference of P between the two sets. For the remaining sections, only ACES results are discussed.

VI.C. Low C-SWaP UAS

Figures 7, 8, and 9 show results of P and MIR for each DWC type. For each DWC type, a DWC that yields the minimum MIR on the contour of 5% P is selected. Such a DWC is marked with a red asterisk.

The MIR for DWC1 and DWC2 becomes independent of τ_{mod} or t_{pz} when their values are small, because HMD* becomes the limiting parameter as the ownship must maneuver away to maintain the HMD* before it goes below the threshold of τ_{mod} or t_{pz}. While DWC1 and DWC2 contours are very similar, DWC2 yields marginally favorable MIR than DWC1. DWC3 results have already been shown in Figure 6 and are not

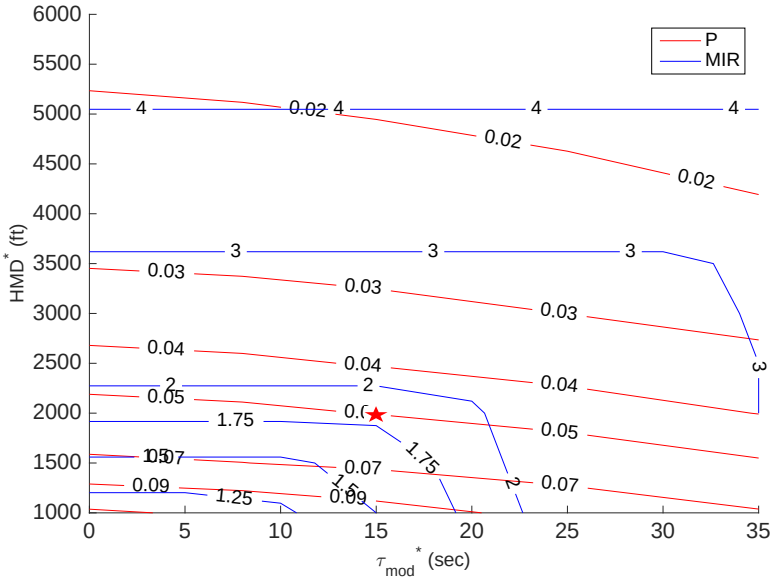

Figure 7. P **and MIR for DWC1. The minimum MIR at 5% P is about 1.8 nmi at 15 sec** τ_{mod} **and 2000 ft HMD.**

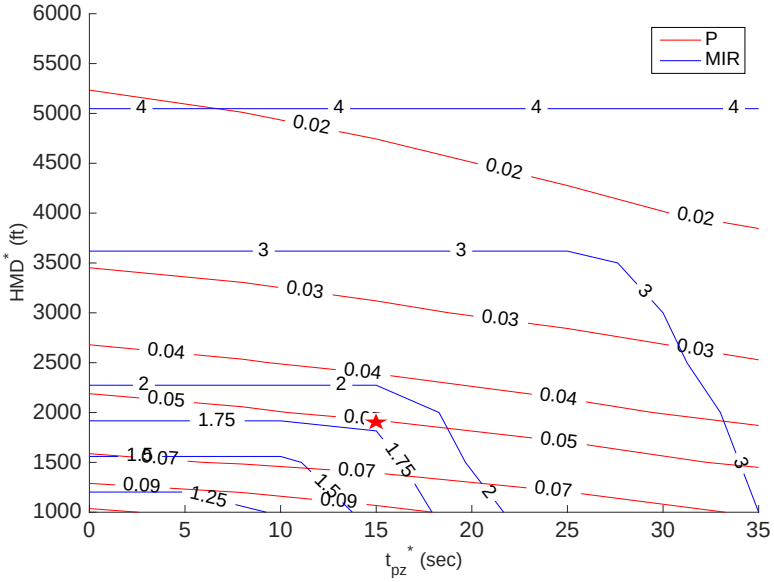

Figure 8. P **and MIR for DWC2. The minimum MIR at 5% P is about 1.8 nmi at 15 sec** t_{pz} **and 2000 ft HMD.**

repeated here. Recall that DWC3's parameter space is a subset of DWC1, DWC2, and DWC4, when their respective time parameter thresholds reduce to zero. The points at which the contours intersect with the vertical axis in Figures 7, 8, and 9 represent DWC3 results and are consistent with the values in Figure 6. DWC4 with $t^* > 0$ leads to unfavorable MIR, and the minimum MIR occurs at $t^* = 0$.

VII. DWC Down-Selection

The DWCs that yield minimum MIR with 5% P are considered as primary candidate DWCs going forward for additional analysis. In addition, it is desirable to select a couple of secondary (backup) candidate DWCs

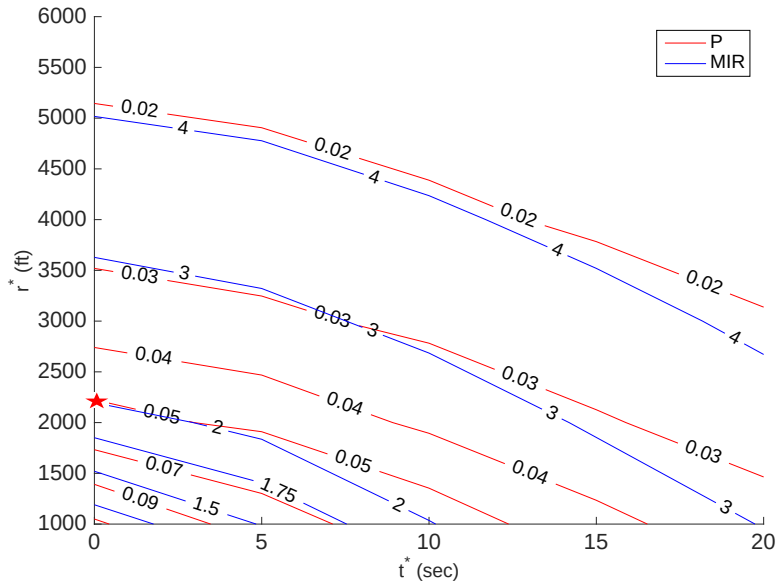

Figure 9. P and MIR for DWC4. The minimum MIR at 5% P is about 2.2 nmi at 0 sec t^* and 2200 ft r^*.

with P under and above 5%, because of the following considerations. The target value of 5% for P is based on a open-loop risk recommendation, not from safety metric evaluation (which will be follow-up work). Without additional analysis, there is no guarantee that 5% for P is low enough. On the other hand, the DAA system might be able to achieve required safety with even higher values of P. Such an option should be explored as an opportunity to enable more UAS operations (with reduced sensor requirements).

Table 4 shows the potential candidate DWCs being considered. The first two definitions are from the DWC1 and DWC2 types that yield the minimum MIR on the 5% contour of P. The third DWC is of the DWC3 type, a cylinder. This DWC is simple since it does not have a time metric. DWC4 is not selected because the added time component worsens MIR performance. Although the second DWC provides the minimum MIR, and it can be argued that t_{pz} serves as a more intuitive time metric for DAA, the second DWC be dropped due to the SC-228 being less familiar with the behavior of t_{pz}. The first and third DWCs are selected as the primary DWCs for future analysis.

Table 4. DWC down-selection

Type	ID	HMD* (or $r*$) (ft)	τ^*_{mod} or t^*_{pz} or t^* (sec)	P (%)	MIR (nmi)	Comment	Selection
DWC1	1	2000	15	5	1.8		Primary
DWC2	2	1950	15	5	1.8		Not selected
DWC3	3	2200	0	5	2.0	simple	Primary
DWC3	4	1200	0	10.0	1.25	terminal WC 1	Not selected
DWC1	5	1500	15	7	1.7	terminal WC 2	Secondary
DWC1	6	2500	25	3.6	2.3	smaller P	Secondary

The fourth and fifth DWCs[28] are two candidate DWCs proposed for terminal area UAS operations. The fourth DWC has been accepted by SC-228 as the terminal WC. However it is fairly small and results in 10.0% of P, deemed too high by the authors. The sixth DWC arises from the authors' consideration to carry forward a DWC with P lower than 5%. This DWC is selected to have a lower P of 3.7% while raising the MIR slighly to 2.3 nmi. The fifth and sixth DWCs are selected as the secondary candidate DWCs.

The four candidate DWCs are shown on Figure 10 as red (primary) and blue (secondary) asterisks in terms of the DWC1 parameter, HMD and τ_{mod}.

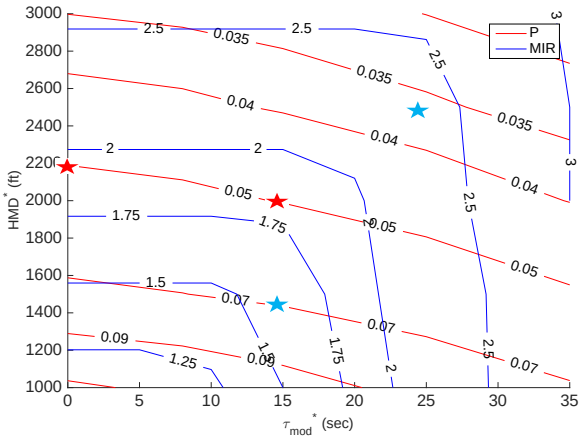

Figure 10. The four candidate DWCs (red for primary and blue for secondary)

VIII. Conclusion and Future Work

This analysis evaluated potential Detect-and-Avoid (DAA) Well Clear (DWC) using two performance metrics, the unmitigated collision risk P and the maneuver initiation range (MIR). Two sets of encounters, one from projected UAS and historical VFR traffic and another from the MIT Lincoln Laboratory uncorrelated encounter model, were used to compute the unmitigated collision risk. The MIR was computed with the anticipated aircraft speed range and turn rate. Based on reasonable values of P and minimum MIR among other considerations, a set of four candidate DWCs, two primary and two secondary, are selected.

Additional analyses will be performed to further differentiate these four candidate DWCs. The final DWC is expected to be applicable to Phase 1 UAS as well, when encountering non-cooperative aircraft. These additional analyses include:

- A trade study between the required sensor surveillance volume and alerting timeline;
- A closed-loop study (using a DAA algorithm to maneuver the UAS away from the intruder) to compute safety metrics such as the risk ratio.

The ultimate goal of this line of research is to provide supporting information for the requirements of low C-SWaP sensors as well as that of alerting and guidance for UAS in encounters with non-cooperative aircraft.

References

[1]Cook, S. P., Brooks, D., Cole, R., Hackenberg, D., and Raska, V., "Defining Well Clear for Unmanned Aircraft Systems," *Proceedings of AIAA Infotech@ Aerospace*, AIAA-2015-0481, AIAA, 2015.

[2]Johnson, M., Mueller, E. R., and Santiago, C., "Characteristics of a Well Clear Definition and Alerting Criteria for Encounters between UAS and Manned Aircraft in Class E Airspace," *Eleventh UAS/Europe Air Traffic Management Research and Development Seminar*, 2015, pp. 23–26.

[3]Walker, D., "FAA Position on Building Consensus Around the SARP Well-Clear Definition," *RTCA Special Committee 228*, 2014.

[4]Murphy, J. R., Hayes, P. S., Kim, S. K., Bridges, W., and Marston, M., "Flight Test Overview for UAS Integration in the NAS Project," *AIAA Atmospheric Flight Mechanics Conference, AIAA SciTech*, AIAA-2016-1756, 2016.

[5]Lee, S. M., Park, C., Thipphavong, D. P., Isaacson, D. R., and Santiago, C., "Evaluating Alerting and Guidance Performance of a UAS Detect-And-Avoid System," NASA/TM-2016-219067, NASA Ames Research Center, 2016.

[6]Smearcheck, S., Calhoun, S., Adams, W., Kresge, J., and Kunzi, F., "Analysis of Alerting Performance for Detect and Avoid of Unmanned Aircraft Systems," *IEEE/ION Position, Location and Navigation Symposium (PLANS)*, 2016, pp. 710–730.

[7]Fern, L., Rorie, R. C., Pack, J. S., Shively, R. J., and Draper, M. H., "An Evaluation of Detect and Avoid (DAA) Displays for Unmanned Aircraft Systems: The Effect of Information Level and Display Location on Pilot Performance," *Proceedings of 15th AIAA Aviation Technology, Integration, and Operations Conference*, AIAA-2015-3327, 2015.

[8]Abramson, M., Refai, M., and Santiago, C., "A Generic Resolution Advisor and Conflict Evaluator (GRACE) in Applications to Detect-And-Avoid (DAA) Systems of Unmanned Aircraft," *Proceedings of the 17th AIAA Aviation Technology, Integration, and Operations (ATIO) Conference*, AIAA-2017-4485, June 2017.

[9]Muñoz, C., Narkawicz, A., Hagen, G., Upchurch, J., Dutle, A., Consiglio, M., and Chamberlain, J., "DAIDALUS: Detect and Avoid Alerting Logic for Unmanned Systems," *34th Digital Avionics Systems Conference (DASC)*, IEEE/AIAA, 2015, pp. 5A1–1.

[10]Suarez, B., Kirk, K., and Theunissen, E., "Development, Integration and Testing of a Stand-Alone CDTI with Conflict Probing Support," *Infotech@ Aerospace 2012*, 2012, p. 2487.

[11]*Minimum Operational Performance Standards (MOPS) for Detect and Avoid (DAA) Systems*, DO-365, RTCA. Inc., 2017.

[12]*Minimum Operational Performance Standards (MOPS) for Air-to-Air Radar for Traffic Surveillance*, DO-366, RTCA. Inc., 2017.

[13]"Introduction to TCAS II Version 7.1," HQ-111358, Federal Aviation Administration (FAA), Feb. 2011.

[14]Ayyalasomayajula, S., Sharma, R., Wieland, F., Trani, A., Hinze, N., and Spencer, S., "UAS Demand Generation Using Subject Matter Expert Interviews and Socio-Economic Analysis," *Proceedings of the AIAA Aviation Conference*, AIAA-2015-3405, 2015.

[15]Weibel, R. E., Edwards, M. W., and Fernandes, C. S., "Establishing a Risk-Based Separation Standard for Unmanned Aircraft Self Separation," *Ninth USA/Europe Air Traffic Management Research & Development Seminar*, 2011.

[16]Jack, D. P., Hoffler, K. D., and Johnson, S., "An Assessment of Unmanned Aircraft System Level-Turn Maneuver Performance Requirements in Relation to a Quantified Well-Clear Definition," *14th AIAA Atmospheric Flight Mechanics Conference*, AIAA-2015-2394, June 2015.

[17]George, S. E., Satapathy, G., Manikonda, V., Refai, M., and Dupee, R., "Build 8 of the Airspace Concept Evaluation System," *AIAA Modeling and Simulation Technologies Conference*, AIAA-2011-6373, Aug. 2011.

[18]Weinert, A. J., Harkleroad, E. P., Griffith, J., Edwards, M. W., and Kochenderfer, M. J., "Uncorrelated Encounter Model of the National Airspace System, Version 2.0," Tech. rep., MIT Lincoln Laboratory, Lexington, Massachusetts, ATC-404, Aug. 2013.

[19]Jack, D. P., Hoffler, K. D., and Johnson, S., "Exploration of the Trade Space Between UAS Maneuver Performance and SAA System Performance Requirements," NASA CR-2014-218264, NASA Langley Research Center, May 2014.

[20]Kochenderfer, M. J., Kuchar, J. K., Espindle, L. P., and Griffith, J., "Uncorrelated Encounter Model of the National Airspace System, Version 1.0," Tech. rep., MIT Lincoln Laboratory, Lexington, Massachusetts, Project Report ATC-345, 2008.

[21]Wu, M. G., Bageshwar, V. L., and Euteneuer, E. A., "An Alternative Time Metric to Modified Tau for Unmanned Aircraft System Detect And Avoid," *17th AIAA Aviation Technology, Integration, and Operations Conference*, AIAA-2017-4383, June 2017.

[22]Nuic, A., Poles, D., and Mouillet, V., "BADA: An Advanced Aircraft Performance Model for Present and Future ATM Systems," *Internaitonal Journal of Adaptive Control and Signal Processing*, Vol. 24, No. 10, 2010, pp. 850 866.

[23]Charvat, R., Ozburn, R., Bushong, S., Cohen, K., and Kumar, M., "SIERRA Team Flight of Zephyr UAS at West Virginia Wild Land Fire Burn," *Infotech@ Aerospace 2012*, AIAA-2012-2544, 2012, p. 2544.

[24]Abramson, M., Refai, M., and Santiago, C., "The Generic Resolution Advisor and Confict Evaluator (GRACE) for Unmanned Aircraft Detect-And-Avoid Systems," NASA/TM-2017-219507, NASA Ames Research Center, 2017.

[25]Kochenderfer, M. J., Espindle, L. P., Kuchar, J. K., and Griffith, J. D., "A Comprehensive Aircraft Encounter Model of the National Airspace System," *Lincoln Laboratory Journal*, Vol. 17, No. 2, 2008.

[26]Jack, D. P., Hardy, J., and Hoffler, K. D., "Analysis of Influence of UAS Speed Range and Turn Performance on Detect and Avoid Sensor Requirements," *18th AIAA Aviation Technology, Integration, and Operations Conference*, AIAA-2018, June 2018.

[27]Hardy, J., Jack, D. P., and Hoffler, K. D., "Sensitivity Analysis of Detect and Avoid Well Clear Parameter Variations on UAS DAA Sensor Requirements," *18th AIAA Aviation Technology, Integration, and Operations Conference*, AIAA-2018, June 2018.

[28]Vincent, M., Trujillo, A., Jack, D., Hoffler, K., and Tsakpinis, D., "A Recommended DAA Well-Clear Definition for the Terminal Environment," *18th AIAA Aviation Technology, Integration, and Operations Conference*, AIAA-2018, June 2018.